ELSEVIER

Inorganica Chimica Acta 225 (1994) 229–238

Inorganica Chimica Acta

Syntheses and structures of mixed-ligand tetrairon–sulfur clusters, $[Cp'_2(Ph_2C_2S_2)_2Fe_4S_4](PF_6)$ and $[Cp'_3(Ph_2C_2S_2)Fe_4S_5](PF_6)_n$ ($n=1$ and 2) ($Cp' = \eta^5$-C_5Me_5). Structural change of the clusters accompanying electron transfer reactions

Shinji Inomata, Keiichi Hitomi, Hiromi Tobita, Hiroshi Ogino*

Department of Chemistry, Faculty of Science, Tohoku University, Sendai 980-77, Japan

Received 10 March 1994

Abstract

The cyclic voltammogram (CV) of the mixed-ligand cubane-type cluster $Cp'_2(Ph_2C_2S_2)_2Fe_4S_4$ (**4**) exhibits four reversible one-electron redox waves, corresponding to $+2/+1$, $+1/0$, $0/-1$, and $-1/-2$ charged cluster couples. The CV of the mixed-ligand cubane-like cluster $Cp'_3(Ph_2C_2S_2)Fe_4S_5$ (**5**) exhibits four reversible one-electron redox waves, corresponding to $+3/+2$, $+2/+1$, $+1/0$, and $0/-1$ charged cluster couples. Oxidized clusters, **[4]**$(PF_6)\cdot CH_2Cl_2$, **[5]**$(PF_6)\cdot 2Me_2CO$ and **[5]**$(PF_6)_2\cdot Me_2CO$, were synthesized by chemical and/or electrochemical methods. The structures of these three salts were determined by X-ray crystallography and compared with those of the parent clusters **4** and **5**. Both clusters **4** and **5** shrink as they are oxidized, indicating that the electrons are removed from antibonding orbitals. The crystallographic data are as follows: **[4]**$(PF_6)\cdot CH_2Cl_2$: orthorhombic, $Pna2_1$ with $a=17.259(3)$, $b=25.682(4)$, $c=12.628(2)$ Å, $V=5597(2)$ Å^3, $Z=4$ and $R=0.066$; **[5]**$(PF_6)\cdot 2Me_2CO$: triclinic, $P\bar{1}$ with $a=14.112(4)$, $b=17.712(3)$, $c=13.325(4)$ Å, $\alpha=108.08(2)$, $\beta=114.74(3)$, $\gamma=84.00(1)°$, $V=2874(1)$ Å^3, $Z=2$ and $R=0.066$; **[5]**$(PF_6)_2\cdot Me_2CO$: triclinic, $P\bar{1}$ with $a=14.985(1)$, $b=15.540(1)$, $c=12.951(1)$ Å, $\alpha=93.40(2)$, $\beta=95.04(1)$, $\gamma=96.76(1)°$, $V=2976(1)$ Å^3, $Z=2$ and $R=0.056$.

Keywords: Crystal structures; Electron transfer; Electrochemistry; Cluster complexes; Iron complexes; Sulfur complexes; Cyclopentadienyl complexes Mixed-ligand tetrairon–sulfur cluster

1. Introduction

The oxidation–reduction (redox) process of a substance is always accompanied by structural change. The investigation, therefore, of the structural change of a substance accompanying redox is of essential importance for understanding electron transfer processes. In this respect, the cubane-type clusters $Cp_4Fe_4S_4$ (**1**) and $Cp_4Fe_4Se_4$ (**2**) provide unique examples. The cyclic voltammogram of each cluster shows four reversible redox waves, indicating the existence of five species **[1]**^{n} or **[2]**^{n} for which $n=0$, $+1$, $+2$, $+3$ and $+4$ [1,2]. The neutral cluster **1** [3] and the salts of **[1]**$^+$ [4], **[1]**$^{2+}$ [5] and **[1]**$^{3+}$ [6] have been isolated and except for the lattermost, their crystal structures have been determined. The selenium cluster **2** [7] and the salts of **[2]**$^+$ [8], **[2]**$^{2+}$ [7] and **[2]**$^{3+}$ [1] have also been isolated and structurally characterized. These studies clearly show that each Fe_4 core of **[1]**^{n} or **[2]**^{n} shrinks with each increase in the charge of the cluster. This arises from the stepwise removal of antibonding electrons from the neutral cluster.

The related clusters $[Cp_4Fe_4S_5]^n$ (**[3]**^{n}; $n=0$, $+1$, $+2$) [9–12] have been isolated and the salts of **[3]**$^+$ [11] and **[3]**$^{2+}$ [12] have been structurally characterized. Each cluster salt contains one S_2 ligand which is coordinated to an iron atom in a 'side-on' mode. The Fe_4 core of **[3]**$^{2+}$ is also smaller than that of **[3]**$^+$.

Recently, we synthesized the mixed-ligand tetrairon–sulfur clusters, $Cp'_2(Ph_2C_2S_2)_2Fe_4S_4$ (**4**) and $Cp'_3(Ph_2C_2S_2)Fe_4S_5$ (**5**), which contain 5-electron donor pentamethylcyclopentadienyl ligands (Cp') and 4-electron donor diphenyldithiolene ligands simultaneously [13–15]. Clusters **4** and **5** have 18 and 19 cluster electrons,

*Corresponding author.

SSDI 0020-1693(94)04051-V

respectively. The molecular structures of **4** and **5** were determined by X-ray crystallography. Cluster **4** is of the cubane-type and there are three Fe–Fe bonds in the Fe_4S_4 core. Cluster **5** contains an Fe_4S_5 core which consists of four iron atoms, three μ_3-S ligands, and an 'end-on' type S_2 ligand. There are two Fe–Fe bonds in the Fe_4S_5 core.

In the present work, the syntheses and crystal structure analyses of the oxidized salts of **4** and **5** were carried out to investigate how **4** and **5** change their structures upon oxidation.

2. Experimental

2.1. Materials

All manipulations were carried out under a dry nitrogen atmosphere. Pentane, hexane, tetrahydrofuran (THF) and diethyl ether were distilled from sodium benzophenone ketyl under a nitrogen atmosphere. Acetone was distilled from anhydrous calcium sulfate. Acetonitrile for electrochemical experiments was distilled twice from phosphorus pentoxide and then from calcium hydride. Dichloromethane was purified by distillation from calcium hydride. The supporting electrolyte in the electrochemical experiments, tetra-n-butylammonium tetrafluoroborate (TBAB), was purchased from Tokyo Chemical Industry Co., Ltd., and purified by recrystallization from benzene/ethyl acetate (10:1 vol./vol.). Ammonium hexafluorophosphate (Aldrich Chemical Co.) was used without further purification. Clusters $Cp'_2(Ph_2C_2S_2)_2Fe_4S_4$ (**4**) and $Cp'_3(Ph_2C_2S_2)Fe_4S_5$ (**5**) were prepared as reported previously [13–15]. The ferrocenium salts $[Cp_2Fe](PF_6)$ and $[(MeC_5H_4)_2Fe](PF_6)$ were prepared by literature methods [16].

2.2. Electrochemical measurements and equipment

Cyclic voltammetry was performed with a normal three-electrode system consisting of a Pt rod electrode as a working electrode, a Pt coil as a counter electrode, and an aqueous saturated calomel electrode (SCE) as a reference electrode. Electrochemical measurements were done using a model 311 potentiostat (Huso Co.) combined with a model 321 function generator (Huso Co.). Bulk electrolysis was performed in a cell which was equipped with a Pt plate electrode as working electrode, a carbon rod as counter electrode and an SCE as reference electrode. The potential was applied by an HA-501 potentiostat (Hokuto Denko Ltd.) coupled with an HB-104 function generator (Hokuto Denko Ltd.).

2.3. Synthesis of $[Cp'_2(Ph_2C_2S_2)_2Fe_4S_4](PF_6)\cdot CH_2Cl_2$ ([4](PF$_6$)·CH$_2$Cl$_2$)

2.3.1. Oxidation of $4\cdot CH_2Cl_2$ with $[Cp_2Fe](PF_6)$

To a CH_2Cl_2 solution (60 ml) of $4\cdot CH_2Cl_2$ (216 mg, 0.18 mmol), was added $[Cp_2Fe](PF_6)$ (94 mg, 0.28 mmol), and the mixture was stirred for 15 min at room temperature. After the solvent was removed by evaporation, the black residue was washed with 100 ml of water and then with 100 ml of hexane. The resulting black powder was dissolved in 15 ml of CH_2Cl_2, and 30 ml of hexane were added carefully. Needle-like crystals of $[4](PF_6)\cdot CH_2Cl_2$ suitable for X-ray analysis were obtained after 24 h. Yield 223 mg (92%). *Anal.* Calc. for $C_{49}H_{52}Cl_2F_6Fe_4PS_8$: C, 44.03; H, 3.92. Found: C, 43.77; H, 3.83%.

2.3.2. Bulk electrolysis of $4\cdot CH_2Cl_2$

Bulk electrolysis of $4\cdot CH_2Cl_2$ (101 mg, 0.085 mmol) was carried out in a mixed solvent of CH_2Cl_2 and CH_3CN (1:1 vol./vol., 100 ml) containing 0.1 M NH_4PF_6 as a supporting electrolyte. The potential was applied at +0.20 V versus SCE and the electrolysis was continued for 2 h. The coulombic number required for the electrolysis was 7.4 C (calc. value 8.2 C). After filtration, the solution was evaporated to dryness. The black residue was washed with 100 ml of water and dried in vacuo. Recrystallization was performed by the same method as that described above. Yield 104 mg (92%).

2.4. Unsuccessful attempt to prepare the dicationic cluster $[Cp'_2(Ph_2C_2S_2)_2Fe_4S_4](PF_6)_2$ ([4](PF$_6$)$_2$)

An acetonitrile solution (100 ml) containing $[4](PF_6)\cdot CH_2Cl_2$ (142 mg, 0.106 mmol) and 0.1 M NH_4PF_6 was electrochemically oxidized at +0.50 V versus SCE for 2 h. The coulombic number required for the electrolysis was 9.9 C (calc. value 10.3 C). After filtration, the solvent was evaporated to dryness and the residue was washed with water to remove the electrolyte. However, the solid was not the dicationic cluster $[4](PF_6)_2$, but the monocationic cluster $[4](PF_6)$.

2.5. Synthesis of $[Cp'_3(Ph_2C_2S_2)Fe_4S_5](PF_6)\cdot 2Me_2CO$ ([5](PF$_6$)·2Me$_2$CO)

To a CH_2Cl_2 solution (50 ml) of **5** (0.196 g, 0.018 mmol) was added 0.090 g (0.25 mmol) of $[(MeC_5H_4)_2Fe](PF_6)$ and the mixture was stirred for 15 min at room temperature. After the solvent was evaporated, the residue was washed with 100 ml of hexane and extracted with acetonitrile. After removal of the solvent, $[5](PF_6)$ was obtained as a dark green powder. Pure crystals of $[5](PF_6)\cdot 2Me_2CO$ suitable for X-ray diffraction were obtained by placing a layer of hexane

Table 1
Crystallographic data for $[Cp'_2(Ph_2C_2S_2)_2Fe_4S_4](PF_6)\cdot CH_2Cl_2$ ([4](PF$_6$)·CH_2Cl_2), $[Cp'_3(Ph_2C_2S_2)Fe_4S_5](PF_6)\cdot 2Me_2CO$ ([5](PF$_6$)·2Me_2CO) and $[Cp'_3(Ph_2C_2S_2)Fe_4S_5](PF_6)_2\cdot Me_2CO$ ([5](PF$_6$)$_2$·Me_2CO)

	[4](PF$_6$)·CH_2Cl_2	[5](PF$_6$)·2Me_2CO	[5](PF$_6$)$_2$·Me_2CO
Formula	$C_{49}H_{52}Cl_2F_6Fe_4PS_8$	$C_{50}H_{67}F_6Fe_4O_2PS_7$	$C_{47}H_{61}F_{12}Fe_4OP_2S_7$
Formula weight	1336.74	1292.90	1379.70
Crystal system	orthorhombic	triclinic	triclinic
Space group	$Pna2_1$	$P\bar{1}$	$P\bar{1}$
a (Å)	17.259(3)	14.112(4)	14.985(1)
b (Å)	25.682(4)	17.712(3)	15.540(1)
c (Å)	12.628(2)	13.325(4)	12.951(1)
α (°)		108.08(2)	93.40(2)
β (°)		114.74(3)	95.04(1)
γ (°)		84.00(2)	96.76(1)
V (Å^3)	5597(2)	2874(1)	2976(1)
Z	4	2	2
λ (Å)	0.71073	0.71073	0.71073
D_{calc} (g cm^{-3})	1.59	1.49	1.54
D_{obs} (g cm^{-3})	1.58	1.49	1.55
Crystal size (mm)	0.60×0.25×0.25	0.60×0.40×0.30	0.50×0.35×0.30
Temperature (°C)	22	21	21
Data collection range, 2θ (°)	3–70	3–60	3–55
μ (Mo Kα) (cm^{-1})	15.1	13.4	13.4
No. unique data, total with $\lvert F_o\rvert > 3\sigma(F_o)$	13356, 6412	16771, 9747	13674, 8823
No. parameters refined	631	562	639
R[a]	0.066	0.066	0.056
R_w[b]	0.075	0.106	0.091

[a] $R = \Sigma\lvert\lvert F_o\rvert - \lvert F_c\rvert\rvert/\Sigma\lvert F_o\rvert$.
[b] $R_w = [\Sigma w(\lvert F_o\rvert - \lvert F_c\rvert)^2/\Sigma w\lvert F_o\rvert^2]^{1/2}$; $w = [\sigma^2(\lvert F_o\rvert) + aF_o^2]^{-1}$, where $a = 0.001$ for [4](PF$_6$)·CH_2Cl_2, 0.003 for [5](PF$_6$)·2Me_2CO, and 0.005 for [5](PF$_6$)$_2$·Me_2CO.

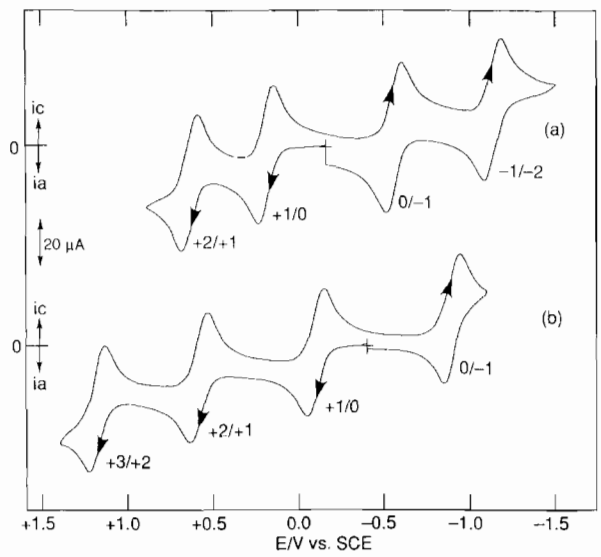

Fig. 1. Cyclic voltammograms of 0.97 mM $Cp'_2(Ph_2C_2S_2)_2Fe_4S_4$ (4) (a) and 1.16 mM $Cp'_3(Ph_2C_2S_2)Fe_4S_5$ (5) (b) in 0.1 M TBAB–CH_2Cl_2 solutions.

over an acetone solution of [5](PF$_6$). Yield 0.195 g (85%). *Anal.* Calc. for $C_{50}H_{67}F_6Fe_4O_2PS_7$: C, 46.45; H, 5.22. Found: C, 46.27; H, 5.01%.

Table 2
Cyclic voltammetric data of 4 and 5 in 0.1 M TBAB–dichloromethane[a]

Cluster	Couple	$E_{1/2}$ vs. SCE (V)	ΔE_p (mV)
4	+2/+1	+0.64	90
	+1/0	+0.20	90
	0/−1	−0.55	100
	−1/−2	−1.13	100
5	+3/+2	+1.19	90
	+2/+1	+0.58	90
	+1/0	−0.14	90
	0/−1	−0.90	90

[a] Sweep rate: 50 mV s^{-1} for 4; 100 mV s^{-1} for 5.

2.6. Synthesis of $[Cp'_3(Ph_2C_2S_2)Fe_4S_5](PF_6)_2\cdot Me_2CO$ ([5](PF$_6$)$_2$·Me_2CO)

Bulk electrolysis of the monocationic cluster [5](PF$_6$)·2Me_2CO (0.147 g, 0.11 mmol) was carried out in an acetonitrile solution (100 ml) containing 0.1 M NH_4PF_6 as supporting electrolyte. The potential was applied at +0.70 V versus SCE and the elcctrolysis was continued for 1 h. The coulombic number required for the electrolysis was 13.6 C (calc. value 11.1 C). After filtration of the solution and removal of the

solvent, the dark green residue was washed with 100 ml of water and dried in vacuo. Single crystals of [5](PF$_6$)$_2$·Me$_2$CO suitable for X-ray diffraction were obtained by layering an acetone solution of [5](PF$_6$) with hexane. Yield 0.128 g (81%). *Anal.* Calc. for $C_{47}H_{61}F_{12}Fe_4OP_2S_7$: C, 40.91; H, 4.46. Found: C, 40.83; H, 4.67%.

2.7. X-ray structural determination of [Cp'$_2$(Ph$_2$C$_2$S$_2$)$_2$Fe$_4$S$_4$](PF$_6$)·CH$_2$Cl$_2$ ([4](PF$_6$)·CH$_2$Cl$_2$), [Cp'$_3$(Ph$_2$C$_2$S$_2$)Fe$_4$S$_5$](PF$_6$)·2Me$_2$CO ([5](PF$_6$)·2Me$_2$CO) and [Cp'$_3$(Ph$_2$C$_2$S$_2$)Fe$_4$S$_5$](PF$_6$)$_2$·Me$_2$CO ([5](PF$_6$)$_2$·Me$_2$CO)

Diffraction data were collected on a Rigaku AFC-6A four-circle diffractometer with graphite-monochromated Mo Kα radiation using the ω scan technique for [4](PF$_6$)·CH$_2$Cl$_2$ and the ω–2θ scan technique for [5](PF$_6$)·2Me$_2$CO and [5](PF$_6$)$_2$·Me$_2$CO. The reflection data were corrected for Lorentz and polarization factors. No correction was applied for absorption. During the data collection, three standard reflections were monitored after every 100 reflections, and no decay was observed. The unit cell dimensions were determined by the least-squares method, using 50 reflections for [4](PF$_6$)·CH$_2$Cl$_2$ and [5](PF$_6$)·2Me$_2$CO and 100 reflections for [5](PF$_6$)$_2$·Me$_2$CO in the range $25 < 2\theta < 30°$.

The structure of [4](PF$_6$)·CH$_2$Cl$_2$ was solved by the heavy atom method. The systematic absence condition *hkl* ($h00$, $h = 2n+1$; $0k0$, $k = 2n+1$; $00l$, $l = 2n+1$; $h0l$, $h = 2n+1$; $0kl$, $k+l = 2n+1$) indicated two possible space groups, $Pna2_1$ and $Pnam$. The space group $Pna2_1$ was later fully confirmed by the successful solution and refinement of the structure. All non-hydrogen atoms were refined by the block-diagonal least-squares method using individual anisotropic thermal parameters. Hydrogen atoms on the four Ph groups were located by calculation (d(C–H) = 1.08 Å). The isotropic thermal parameters of the hydrogen atoms were fixed at 1.5

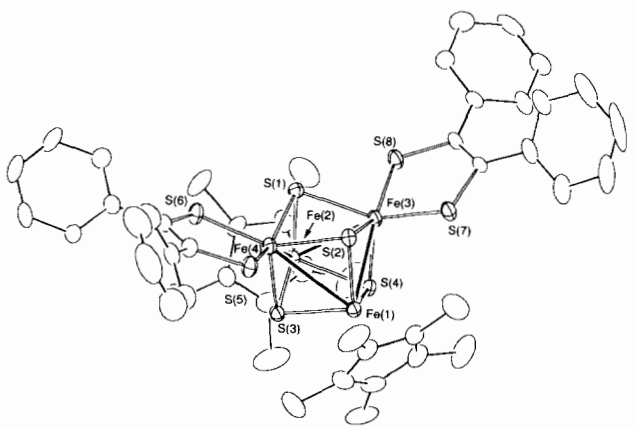

Fig. 2. ORTEP drawing of the cationic moiety in [4](PF$_6$). Thermal ellipsoids are at 30% probability.

Table 3
Final atomic coordinates ($\times 10^4$) and equivalent isotropic temperature factors for [Cp'$_2$(Ph$_2$C$_2$S$_2$)$_2$Fe$_4$S$_4$](PF$_6$)·CH$_2$Cl$_2$ ([4](PF$_6$)·CH$_2$Cl$_2$)

Atom	x	y	z	B_{eq}[a] (Å^2)
Fe(1)	1164.5(6)	−9.6(4)	−180(1)	2.4
Fe(2)	2863.2(6)	63.9(3)	930(1)	2.3
Fe(3)	1680.1(6)	−611.5(3)	1500	2.5
Fe(4)	1587.8(6)	641.3(3)	1553(1)	2.5
S(1)	2253(1)	29.3(7)	2432(2)	2.6
S(2)	713(1)	−14.6(7)	1441(2)	2.6
S(3)	2094(1)	591.6(6)	0(2)	2.5
S(4)	2205(1)	−518.0(6)	−21(2)	2.5
S(5)	623(1)	1171.7(7)	1427(2)	3.4
S(6)	2142(1)	1222.7(7)	2550(2)	3.4
S(7)	789(1)	−1200.6(7)	1397(2)	3.3
S(8)	2309(1)	−1155.5(7)	2491(2)	3.5
C(1)	1121(6)	−24(4)	−1847(8)	4.3
C(2)	691(5)	416(4)	−1506(8)	4.4
C(3)	62(5)	235(4)	−889(8)	4.0
C(4)	118(5)	−333(4)	−867(8)	4.1
C(5)	761(6)	−489(4)	−1451(8)	4.7
C(6)	3834(5)	192(4)	−67(9)	4.6
C(7)	3829(5)	581(3)	719(8)	3.7
C(8)	3920(4)	327(4)	1701(7)	3.6
C(9)	3969(4)	−214(3)	1521(9)	3.8
C(10)	3925(4)	−306(4)	415(9)	4.3
C(11)	1808(7)	−7(5)	−2571(9)	6.9
C(12)	823(7)	982(4)	−1756(11)	7.2
C(13)	−606(6)	536(5)	−439(10)	6.8
C(14)	−515(7)	−683(5)	−382(12)	8.2
C(15)	984(8)	−1063(5)	−1659(12)	8.6
C(16)	3825(7)	297(8)	−1264(11)	8.8
C(17)	3814(7)	1162(4)	528(12)	7.0
C(18)	4006(6)	598(5)	2801(10)	6.2
C(19)	4130(7)	−614(5)	2389(14)	8.4
C(20)	4029(7)	−819(6)	−122(14)	8.5
C(21)	831(5)	1728(3)	2138(7)	3.1
C(22)	1533(5)	1753(3)	2650(7)	2.9
C(23)	1059(5)	−1732(3)	2136(7)	2.9
C(24)	1776(4)	−1716(2)	2628(7)	2.8
C(25)	190(5)	2107(3)	2223(8)	3.8
C(26)	−22(6)	2316(4)	3195(10)	5.2
C(27)	−675(7)	2634(4)	3263(12)	7.4
C(28)	−1104(7)	2728(4)	2421(16)	9.2
C(29)	−932(7)	2524(5)	1379(13)	8.0
C(30)	−267(7)	2209(4)	1333(10)	5.8
C(31)	1824(5)	2200(3)	3290(7)	3.5
C(32)	1772(6)	2712(3)	2917(8)	3.9
C(33)	2077(7)	3117(3)	3526(10)	5.4
C(34)	2414(7)	3016(4)	4486(10)	6.0
C(35)	2452(7)	2525(4)	4874(10)	6.3
C(36)	2156(7)	2109(4)	4254(9)	5.0
C(37)	476(5)	−2152(3)	2240(9)	4.3
C(38)	64(6)	−2307(4)	1342(12)	6.5
C(39)	−542(7)	−2674(4)	1504(16)	9.2
C(40)	−713(7)	−2870(4)	2453(18)	11.0
C(41)	−293(7)	−2726(4)	3319(13)	8.2
C(42)	290(6)	−2359(4)	3225(10)	5.3
C(43)	2121(5)	−2123(3)	3313(7)	3.4
C(44)	2096(6)	−2648(3)	2955(9)	4.6
C(45)	2457(7)	−3021(3)	3598(9)	5.2
C(46)	2813(7)	−2895(4)	4496(10)	6.1
C(47)	2841(8)	−2377(4)	4866(10)	6.4
C(48)	2494(6)	−1998(4)	4240(8)	4.6

(*continued*)

Table 3 (*continued*)

Atom	x	y	z	B_{eq}[a] (Å^2)
P	1238(2)	4249(2)	826(4)	7.5
F(1)	1855(7)	3861(6)	1178(13)	18.6
F(2)	621(6)	4596(5)	361(13)	17.6
F(3)	989(9)	3864(5)	−6(13)	19.8
F(4)	1545(9)	4643(7)	1598(14)	22.6
F(5)	648(7)	4051(7)	1604(11)	18.7
F(6)	1812(6)	4472(6)	24(12)	17.1
C(49)	3529(12)	881(8)	5598(21)	15.4
Cl(1)	2583(5)	991(4)	5855(11)	30.3
Cl(2)	3993(3)	1341(2)	6037(13)	24.8

[a]The equivalent isotropic temperature factors for non-hydrogen atoms were computed using the following expression: $B_{eq} = 4/3(B_{11}a^2 + B_{22}b^2 + B_{33}c^2)$. B_{ij} is defined by $\exp[-(h^2B_{11} + k^2B_{22} + l^2B_{33} + 2hkB_{12} + 2hlB_{13} + 2klB_{23})]$.

Table 4
Selected interatomic distances (Å) and angles (°) for $[Cp'_2(Ph_2C_2S_2)_2Fe_4S_4](PF_6)\cdot CH_2Cl_2$ ([**4**](PF$_6$)·CH$_2$Cl$_2$)

Fe(1)···Fe(2)	3.255(2)	Fe(1)–Fe(3)	2.772(1)
Fe(1)–Fe(4)	2.849(2)	Fe(2)–Fe(3)	2.774(1)
Fe(2)–Fe(4)	2.768(1)	Fe(3)···Fe(4)	3.222(1)
Fe(1)–S(2)	2.190(3)	Fe(1)–S(3)	2.238(2)
Fe(1)–S(4)	2.229(2)	Fe(2)–S(1)	2.172(2)
Fe(2)–S(3)	2.231(2)	Fe(2)–S(4)	2.228(2)
Fe(3)–S(1)	2.252(2)	Fe(3)–S(2)	2.268(2)
Fe(3)–S(4)	2.137(2)	Fe(3)–S(7)	2.161(2)
Fe(3)–S(8)	2.167(2)	Fe(4)–S(1)	2.241(2)
Fe(4)–S(2)	2.267(2)	Fe(4)–S(3)	2.150(3)
Fe(4)–S(5)	2.157(2)	Fe(4)–S(6)	2.175(2)
S(5)–C(21)	1.724(8)	S(6)–C(22)	1.725(7)
S(7)–C(23)	1.717(8)	S(8)–C(24)	1.715(7)
C(21)–C(22)	1.375(12)	C(23)–C(24)	1.386(11)
S(2)–Fe(1)–S(4)	101.47(9)	S(2)–Fe(1)–S(3)	99.45(9)
S(3)–Fe(1)–S(4)	79.50(7)	S(1)–Fe(2)–S(4)	101.29(8)
S(1)–Fe(2)–S(3)	101.29(8)	S(3)–Fe(2)–S(4)	79.66(8)
S(1)–Fe(3)–S(4)	101.62(8)	S(1)–Fe(3)–S(2)	81.18(7)
S(2)–Fe(3)–S(4)	101.91(8)	S(7)–Fe(3)–S(8)	86.55(8)
S(1)–Fe(4)–S(2)	81.44(7)	S(1)–Fe(4)–S(3)	101.66(9)
S(2)–Fe(4)–S(3)	99.77(9)	S(5)–Fe(4)–S(6)	87.04(8)
Fe(2)–S(1)–Fe(3)	77.66(8)	Fe(2)–S(1)–Fe(4)	77.69(8)
Fe(3)–S(1)–Fe(4)	91.63(8)	Fe(1)–S(2)–Fe(3)	76.86(8)
Fe(1)–S(2)–Fe(4)	79.43(8)	Fe(3)–S(2)–Fe(4)	90.56(7)
Fe(1)–S(3)–Fe(4)	80.95(8)	Fe(1)–S(3)–Fe(2)	93.50(7)
Fe(2)–S(3)–Fe(4)	78.36(8)	Fe(1)–S(4)–Fe(2)	93.82(7)
Fe(2)–S(4)–Fe(3)	78.91(8)	Fe(3)–S(4)–Fe(1)	78.79(7)
Fe(4)–S(5)–C(21)	108.9(3)	Fe(4)–S(6)–C(22)	108.5(3)
Fe(3)–S(7)–C(23)	109.3(3)	Fe(3)–S(8)–C(24)	109.3(3)
S(5)–C(21)–C(22)	117.9(6)	S(6)–C(22)–C(21)	117.7(6)
S(7)–C(23)–C(24)	117.6(6)	S(8)–C(24)–C(23)	117.3(6)

times the equivalent thermal parameters of the carbon atoms to which they are covalently bonded. Determination of the absolute configuration was carried out by refinement with anomalous dispersion parameters. The inverse chirality of [**4**](PF$_6$)·CH$_2$Cl$_2$ gave a larger R value (0.0687) than that for the adopted chirality.

The structure of [**5**](PF$_6$)·2Me$_2$CO was solved by the direct method (MULTAN), which afforded the positions

Table 5
Final atomic coordinates ($\times 10^4$) and equivalent isotropic temperature factors for $[Cp'_3(Ph_2C_2S_2)Fe_4S_5](PF_6)\cdot 2Me_2CO$ ([**5**](PF$_6$)·2Me$_2$CO)

Atom	x	y	z	B_{eq}[a] (Å^2)
Fe(1)	2566.4(6)	3307.6(4)	666.5(6)	3.6
Fe(2)	867.7(6)	2631.5(4)	582.7(6)	3.4
Fe(3)	483.3(6)	2689.0(4)	−2363.9(6)	3.7
Fe(4)	1910.4(6)	1763.6(4)	−740.6(7)	4.1
S(1)	215.5(10)	2051.5(7)	−1344.8(10)	3.6
S(2)	2141.0(10)	2801.0(7)	−1243.5(11)	3.8
S(3)	2472.8(10)	2240.7(8)	1098.4(12)	4.1
S(4)	165.4(11)	3829.1(7)	−1329.1(11)	4.1
S(5)	974.4(10)	3813.8(7)	336.2(10)	3.7
S(6)	1356.8(11)	531.0(8)	−1219.7(14)	4.6
S(7)	3251.2(11)	1255.7(8)	−1132.4(14)	4.5
C(1)	3805(5)	3812(5)	2364(6)	6.3
C(2)	4238(5)	3387(4)	1572(6)	5.7
C(3)	3969(6)	3740(5)	718(6)	6.7
C(4)	3309(6)	4364(4)	899(7)	7.3
C(5)	3244(5)	4411(4)	1931(8)	8.2
C(6)	4107(8)	3607(9)	3492(8)	11.9
C(7)	4985(6)	2701(6)	1689(13)	12.1
C(8)	4386(8)	3535(9)	−191(9)	12.3
C(9)	2822(11)	4927(7)	181(14)	18.0
C(10)	2740(9)	5046(7)	2660(14)	17.6
C(11)	908(6)	2656(4)	2241(5)	5.9
C(12)	219(7)	3231(4)	1823(6)	6.4
C(13)	−590(6)	2818(5)	736(7)	6.5
C(14)	−392(5)	1988(4)	531(5)	5.1
C(15)	530(5)	1901(3)	1429(6)	4.9
C(16)	1878(9)	2744(8)	3398(7)	10.9
C(17)	293(11)	4096(5)	2495(11)	12.3
C(18)	−1520(7)	3193(8)	−26(11)	11.0
C(19)	−1066(8)	1302(6)	−390(8)	9.4
C(20)	1045(8)	1118(5)	1626(11)	9.5
C(21)	70(6)	3068(3)	−3860(5)	5.6
C(22)	−806(5)	2707(4)	−3937(5)	5.9
C(23)	−585(5)	1909(4)	−3950(5)	5.4
C(24)	439(5)	1773(4)	−3880(5)	5.0
C(25)	850(5)	2477(4)	−3834(5)	5.3
C(26)	138(9)	3890(5)	−3913(7)	8.8
C(27)	−1848(8)	3078(7)	−4076(8)	10.5
C(28)	−1332(7)	1281(6)	−4065(7)	9.1
C(29)	971(8)	989(5)	−3940(7)	8.4
C(30)	1923(7)	2579(6)	−3819(7)	8.3
C(31)	2260(4)	−95(3)	−1601(4)	3.9
C(32)	3118(4)	229(3)	−1548(4)	3.8
C(33)	2010(4)	−963(3)	−1952(4)	3.8
C(34)	1058(5)	−1271(4)	−2819(5)	4.9
C(35)	830(6)	−2095(4)	−3168(6)	6.5
C(36)	1565(6)	−2592(4)	−2641(7)	6.0
C(37)	2474(6)	−2276(4)	−1779(7)	6.1
C(38)	2727(5)	−1473(4)	−1404(6)	5.5
C(39)	3909(4)	−215(3)	−1946(4)	3.9
C(40)	3620(5)	−846(4)	−2976(5)	4.9
C(41)	4356(5)	−1224(4)	−3363(6)	5.9
C(42)	5414(6)	−1030(4)	−2718(7)	6.2
C(43)	5709(5)	−419(5)	−1707(7)	6.0
C(44)	4964(4)	−11(4)	−1319(5)	5.0
P	3103(2)	5090(1)	−3346(2)	7.5
F(1)	2878(9)	4329(7)	−4270(11)	19.3*
F(2)	1912(8)	5238(6)	−3701(9)	18.1*
F(3)	3002(8)	4477(7)	−2763(10)	18.5*
F(4)	3179(9)	5799(8)	−3713(11)	21.8*

(*continued*)

Table 5 (*continued*)

Atom	x	y	z	B_{eq}[a] (Å^2)
F(5)	4307(9)	4983(7)	−2914(10)	19.4*
F(6)	3401(9)	5825(7)	−2152(10)	19.3*
O	6260(11)	2285(9)	−3153(13)	20.5*
C(45)	5416(21)	2833(17)	−2895(25)	26.8*
C(46)	4991(17)	2978(13)	−3989(20)	20.7*
C(47)	5466(23)	2296(19)	−2336(28)	30.0*
OC1[b]	3091(15)	−240(12)	−6452(18)	24.1*
OC2[b]	3410(19)	1250(16)	−5173(23)	31.5*
C(48)	2912(23)	434(17)	−5522(26)	27.3*
C(49)	3886(16)	583(13)	−4287(19)	19.2*

[a]The equivalent isotropic temperature factors for non-hydrogen atoms were computed using the following expression: $B_{eq} = 4/3(B_{11}a^2 + B_{22}b^2 + B_{33}c^2 + B_{12}ab \cos\gamma + B_{13}ac \cos\beta + B_{23}bc \cos\alpha)$. B_{ij} is defined by $\exp[-(h^2B_{11} + k^2B_{22} + l^2B_{33} + 2hkB_{12} + 2hlB_{13} + 2klB_{23})]$.

[b]OC1, OC2 = 0.5 (O + C). Starred atoms were refined isotropically.

Table 6
Selected interatomic distances (Å) and angles (°) for $[Cp'_3(Ph_2C_2S_2)Fe_4S_5](PF_6)\cdot 2Me_2CO$ ([**5**](PF$_6$)·2Me$_2$CO)

Fe(1)–Fe(2)	2.736(2)	Fe(1)···Fe(3)	3.760(2)
Fe(1)–Fe(4)	2.783(1)	Fe(2)···Fe(3)	3.765(2)
Fe(2)–Fe(4)	2.767(2)	Fe(3)···Fe(4)	3.047(2)
Fe(1)–S(2)	2.249(2)	Fe(1)–S(3)	2.170(2)
Fe(1)–S(5)	2.245(2)	Fe(2)–S(1)	2.254(2)
Fe(2)–S(3)	2.179(2)	Fe(2)–S(5)	2.247(2)
Fe(3)–S(1)	2.175(2)	Fe(3)–S(2)	2.175(2)
Fe(3)–S(4)	2.186(2)	Fe(4)–S(1)	2.240(2)
Fe(4)–S(2)	2.237(2)	Fe(4)–S(3)	2.139(2)
Fe(4)–S(6)	2.204(2)	Fe(4)–S(7)	2.200(2)
S(4)–S(5)	2.034(2)	S(6)–C(31)	1.734(6)
S(7)–C(32)	1.735(5)	C(31)–C(32)	1.360(9)
S(2)–Fe(1)–S(5)	91.12(6)	S(2)–Fe(1)–S(3)	100.47(7)
S(3)–Fe(1)–S(5)	103.30(7)	S(1)–Fe(2)–S(3)	101.14(6)
S(1)–Fe(2)–S(5)	90.72(6)	S(3)–Fe(2)–S(5)	102.96(6)
S(1)–Fe(3)–S(2)	90.22(6)	S(1)–Fe(3)–S(4)	91.92(7)
S(2)–Fe(3)–S(4)	92.36(5)	S(1)–Fe(4)–S(2)	87.02(6)
S(1)–Fe(4)–S(3)	102.85(7)	S(2)–Fe(4)–S(3)	101.85(7)
S(6)–Fe(4)–S(7)	86.88(7)		
Fe(3)–S(1)–Fe(4)	87.27(7)	Fe(2)–S(1)–Fe(3)	116.41(6)
Fe(2)–S(1)–Fe(4)	75.99(5)	Fe(1)–S(2)–Fe(3)	116.39(8)
Fe(1)–S(2)–Fe(4)	76.69(7)	Fe(3)–S(2)–Fe(4)	87.36(6)
Fe(1)–S(3)–Fe(2)	77.97(6)	Fe(1)–S(3)–Fe(4)	80.45(8)
Fe(2)–S(3)–Fe(4)	79.69(5)	Fe(1)–S(5)–Fe(2)	75.04(5)
Fe(2)–S(5)–S(4)	113.08(7)	Fe(1)–S(5)–S(4)	112.89(9)
Fe(4)–S(6)–C(31)	107.7(2)	Fe(4)–S(7)–C(32)	107.9(2)
S(6)–C(31)–C(32)	119.0(4)	S(7)–C(32)–C(31)	118.5(4)

of the four iron atoms and seven sulfur atoms. All remaining non-hydrogen atoms except two acetone molecules and fluorine atoms in the PF_6^- anion were refined by the block-diagonal least-squares method with anisotropic thermal parameters. One of the acetone molecules was disordered. The atoms in two acetone molecules and fluorine atoms in PF_6^- anion were isotropically refined. Hydrogen atoms on the two Ph groups were located by calculation (d(C–H) = 1.08 Å).

Table 7
Final atomic coordinates (×10^4) and equivalent isotropic temperature factors for $[Cp'_3(Ph_2C_2S_2)Fe_4S_5](PF_6)_2\cdot Me_2CO$ ([**5**](PF$_6$)$_2$·Me$_2$CO)

Atom	x	y	z	B_{eq}[a] (Å^2)
Fe(1)	3476.0(5)	2588.6(5)	1316.4(5)	2.8
Fe(2)	3389.5(4)	2550.2(4)	3394.9(5)	2.7
Fe(3)	2379.0(5)	4438.3(5)	2378.8(5)	3.0
Fe(4)	1863.0(5)	2529.1(5)	2107.6(5)	3.0
S(1)	2334.3(8)	3454.0(8)	3498.9(9)	2.9
S(2)	2440.5(8)	3507.7(9)	1070.6(9)	3.0
S(3)	2799.0(9)	1587.5(8)	2171.9(9)	3.2
S(4)	3849.2(9)	4697.2(8)	2610.6(11)	3.5
S(5)	4262.6(8)	3504.6(8)	2566.3(9)	3.0
S(6)	734.1(9)	2116.2(11)	3006.2(11)	4.1
S(7)	944.7(9)	2065.1(11)	728.3(10)	4.2
C(1)	3383(5)	1733(5)	−80(5)	6.1
C(2)	4156(6)	1600(5)	556(5)	6.0
C(3)	4711(4)	2383(7)	676(5)	7.5
C(4)	4253(6)	3001(4)	100(6)	6.8
C(5)	3464(6)	2550(6)	−352(5)	6.5
C(6)	2669(9)	988(10)	−428(10)	13.6
C(7)	4397(12)	759(8)	919(9)	14.3
C(8)	5671(7)	2526(16)	1198(10)	19.7
C(9)	4608(14)	3926(7)	−49(13)	18.9
C(10)	2844(11)	2938(12)	−1152(7)	15.0
C(11)	3232(5)	1595(5)	4540(5)	5.3
C(12)	3202(4)	2403(5)	5026(4)	4.9
C(13)	4017(5)	2927(4)	4932(4)	4.7
C(14)	4586(4)	2408(5)	4395(5)	5.0
C(15)	4068(6)	1587(5)	4168(5)	6.1
C(16)	2525(9)	829(7)	4490(8)	11.4
C(17)	2468(7)	2666(9)	5654(6)	9.5
C(18)	4303(8)	3852(6)	5388(6)	8.8
C(19)	5567(5)	2630(9)	4216(7)	9.9
C(20)	4409(11)	762(8)	3709(7)	13.1
C(21)	2328(5)	5796(5)	2153(7)	6.1
C(22)	1700(6)	5287(6)	1433(5)	6.4
C(23)	1033(4)	4771(5)	2011(5)	5.0
C(24)	1301(4)	5000(4)	3073(5)	4.5
C(25)	2092(5)	5618(5)	3152(6)	5.7
C(26)	3058(8)	6446(6)	1882(14)	13.3
C(27)	1660(9)	5300(9)	264(6)	11.8
C(28)	200(5)	4158(7)	1628(9)	9.3
C(29)	809(7)	4725(7)	3961(7)	8.6
C(30)	2601(9)	6050(8)	4168(10)	13.2
C(31)	−170(4)	1700(4)	2159(4)	3.9
C(32)	−85(3)	1680(4)	1113(4)	3.7
C(33)	−1023(4)	1411(4)	2618(5)	4.2
C(34)	−1427(5)	2007(5)	3203(8)	6.7
C(35)	−2231(6)	1714(6)	3633(9)	8.5
C(36)	−2611(5)	888(7)	3479(7)	7.5
C(37)	−2239(5)	316(5)	2902(6)	6.7
C(38)	−1429(5)	556(5)	2460(6)	5.8
C(39)	−812(4)	1392(4)	259(5)	4.4
C(40)	−661(5)	846(5)	−571(6)	5.5
C(41)	−1308(6)	604(6)	−1388(6)	6.8
C(42)	−2119(5)	942(6)	−1398(7)	7.6
C(43)	−2295(5)	1491(6)	−598(7)	6.6
C(44)	−1640(4)	1725(5)	263(6)	5.4
P(1)	4903(1)	1477(1)	7400(1)	4.5
P(2)	2379(2)	5461(2)	7316(2)	6.4
F(1)	5260(4)	2074(4)	8414(4)	9.1
F(2)	3937(5)	1792(5)	7375(6)	12.7
F(3)	5206(6)	2226(5)	6715(5)	12.3

(*continued*)

Table 7 (*continued*)

Atom	x	y	z	B_{eq}[a] (Å^2)
F(4)	4515(6)	739(5)	8081(6)	13.4
F(5)	5827(4)	1130(5)	7434(5)	11.7
F(6)	4549(4)	899(4)	6380(4)	9.0
F(7)	1575(5)	5758(5)	6616(5)	12.0
F(8)	2999(5)	6135(6)	6869(6)	14.3
F(9)	2202(7)	6141(5)	8164(5)	13.6
F(10)	2445(8)	4802(6)	6398(7)	17.2
F(11)	1684(6)	4801(5)	7823(6)	14.7
F(12)	3135(6)	5187(7)	8034(8)	18.1
O	45(11)	2982(11)	8081(13)	22.5*
C(45)	624(14)	2004(13)	7344(15)	17.3*
C(46)	−270(35)	2359(36)	6865(42)	46.6*
C(47)	−9(29)	2934(30)	6295(36)	37.9*

[a]The equivalent isotropic temperature factors for non-hydrogen atoms were computed using the following expression: $B_{eq} = 4/3(B_{11}a^2 + B_{22}b^2 + B_{33}c^2 + B_{12}ab\cos\gamma + B_{13}ac\cos\beta + B_{23}bc\cos\alpha)$. The B_{ij} is defined by $\exp[-(h^2B_{11} + k^2B_{22} + l^2B_{33} + 2hkB_{12} + 2hlB_{13} + 2klB_{23})]$. Starred atoms were refined isotropically.

Table 8
Selected interatomic distances (Å) and angles (°) for $[Cp'_3(Ph_2C_2S_2)Fe_4S_5](PF_6)_2 \cdot Me_2CO$ ([5]$(PF_6)_2 \cdot Me_2CO$)

Fe(1)–Fe(2)	2.710(1)	Fe(1)···Fe(3)	3.728(1)
Fe(1)–Fe(4)	2.701(1)	Fe(2)···Fe(3)	3.713(1)
Fe(2)–Fe(4)	2.705(1)	Fe(3)–Fe(4)	2.969(1)
Fe(1)–S(2)	2.245(2)	Fe(1)–S(3)	2.170(2)
Fe(1)–S(5)	2.243(2)	Fe(2)–S(1)	2.243(1)
Fe(2)–S(3)	2.166(2)	Fe(2)–S(5)	2.245(2)
Fe(3)–S(1)	2.169(2)	Fe(3)–S(2)	2.177(2)
Fe(3)–S(4)	2.183(2)	Fe(4)–S(1)	2.245(2)
Fe(4)–S(2)	2.236(2)	Fe(4)–S(3)	2.143(2)
Fe(4)–S(6)	2.192(2)	Fe(4)–S(7)	2.188(2)
S(4)–S(5)	2.021(2)	S(6)–C(31)	1.704(6)
S(7)–C(32)	1.715(6)	C(31)–C(32)	1.371(10)
S(2)–Fe(1)–S(5)	91.21(6)	S(2)–Fe(1)–S(3)	103.23(6)
S(3)–Fe(1)–S(5)	103.61(6)	S(1)–Fe(2)–S(3)	103.25(5)
S(1)–Fe(2)–S(5)	91.79(5)	S(3)–Fe(2)–S(5)	103.67(6)
S(1)–Fe(3)–S(2)	93.61(6)	S(1)–Fe(3)–S(4)	92.59(6)
S(2)–Fe(3)–S(4)	91.51(6)	S(1)–Fe(4)–S(2)	89.97(6)
S(1)–Fe(4)–S(3)	103.90(6)	S(2)–Fe(4)–S(3)	104.38(6)
S(6)–Fe(4)–S(7)	86.16(7)		
Fe(3)–S(1)–Fe(4)	84.50(6)	Fe(2)–S(1)–Fe(3)	114.63(7)
Fe(2)–S(1)–Fe(4)	74.14(5)	Fe(1)–S(2)–Fe(3)	114.95(7)
Fe(1)–S(2)–Fe(4)	74.13(6)	Fe(3)–S(2)–Fe(4)	84.53(7)
Fe(1)–S(3)–Fe(2)	77.38(5)	Fe(1)–S(3)–Fe(4)	77.55(5)
Fe(2)–S(3)–Fe(4)	77.78(5)	Fe(1)–S(5)–Fe(2)	74.28(4)
Fe(2)–S(5)–S(4)	112.64(7)	Fe(1)–S(5)–S(4)	112.66(7)
Fe(4)–S(6)–C(31)	108.4(2)	Fe(4)–S(7)–C(32)	108.9(2)
S(6)–C(31)–C(32)	119.1(5)	S(7)–C(32)–C(31)	117.5(5)

The isotropic thermal values were fixed by the same method as that for [4]$(PF_6) \cdot CH_2Cl_2$.

The structure of [5]$(PF_6)_2 \cdot Me_2CO$ was solved by the heavy atom method, which provided the positions of the four iron atoms. All remaining non-hydrogen atoms except for the acetone molecule were refined by the block-diagonal least-squares method with anisotropic thermal parameters. Hydrogen atoms on the two Ph groups were located by calculation (d(C–H) = 1.08 Å). The isotropic thermal values were fixed by the same method as that for [4]$(PF_6) \cdot CH_2Cl_2$.

Values for the atomic scattering factors of the non-hydrogen and hydrogen atoms were taken from Refs.[17] and [18], respectively. Calculations were performed on a Nippon Electric Co. ACOS-2000 or ACOS-3900 computer at Tohoku University Computer Center using the Universal Computation Program System UNICS III [19]. Crystallographic data for the clusters [4]$(PF_6) \cdot CH_2Cl_2$, [5]$(PF_6) \cdot 2Me_2CO$ and [5]$(PF_6)_2 \cdot Me_2CO$ are listed in Table 1.

3. Results and discussion

3.1. Electrochemistry of $Cp'_2(Ph_2C_2S_2)_2Fe_4S_4$ (4) and $Cp'_3(Ph_2C_2S_2)Fe_4S_5$ (5)

The cyclic voltammograms of the mixed-ligand tetrairon–sulfur clusters $Cp'_2(Ph_2C_2S_2)_2Fe_4S_4$ (**4**) and $Cp'_3(Ph_2C_2S_2)Fe_4S_5$ (**5**) are shown in Fig. 1. The values of the half-wave potentials ($E_{1/2}$) and peak separation between anodic and cathodic peak potentials (ΔE_p) for **4** and **5** are summarized in Table 2. The cyclic voltammogram of **4** exhibits four reversible one-electron redox waves, corresponding to +2/+1, +1/0, 0/−1 and −1/−2 charged couples. According to the cluster electron counting rules for cubane-type clusters [5,13,20], cluster **4** has 18 cluster electrons. The cyclic voltammogram observed for **4** thus corresponds to a change in the number of cluster electrons from 16 to 20. This change is the same as those observed for $Cp^*_4Fe_4S_4$ ($Cp^* = Cp$ [1,2], MeC_5H_4 [21]), $Cp_4Fe_4Se_4$ [1] and $L_4Fe_4S_4$ ($L = Ph_2C_2S_2$, $(CF_3)_2C_2S_2$) [22].

The cyclic voltammogram of **5**, which has 19 cluster electrons, also exhibits four reversible one-electron redox waves, indicating the existence of five discrete species $[Cp'_3(Ph_2C_2S_2)Fe_4S_5]^n$ (n = +3, +2, +1, 0 and −1). This change in total charge also corresponds to a change in the number of cluster electrons from 16 to 20.

3.2. Isolation of oxidation products of 4 and 5

The monocationic cluster $[Cp'_2(Ph_2C_2S_2)_2Fe_4S_4](PF_6)$ ([4](PF_6)) was prepared by two methods: bulk electrolysis of **4** and chemical oxidation of **4** with $[Cp_2Fe](PF_6)$. The preparation of the dicationic cluster [4]$(PF_6)_2$ failed since the dication produced by bulk electrolysis was too easily reduced to the monocation. A similar observation has been reported for $[Cp_4Fe_4S_4]^{3+}$ [6].

The preparation of the monocationic cluster $[Cp'_3(Ph_2C_2S_2)Fe_4S_5](PF_6)$ ([5](PF_6)) was achieved by the chemical oxidation of neutral cluster **5** with

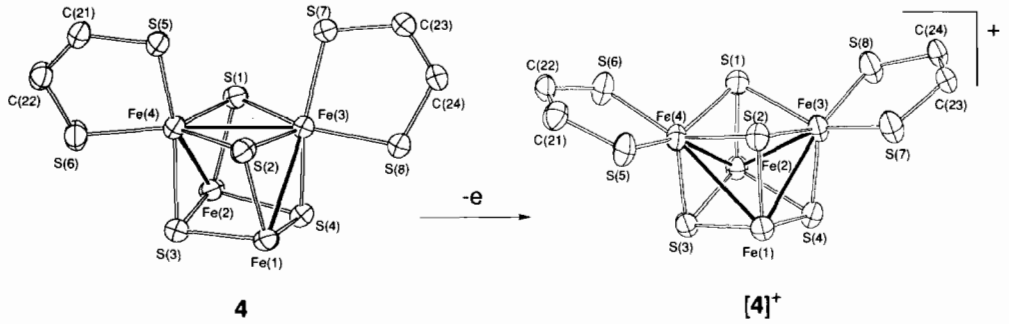

4 $[4]^+$

Fig. 3. Structural change of **4** accompanying one-electron oxidation. Cp', Ph groups and counter anions are omitted for clarity.

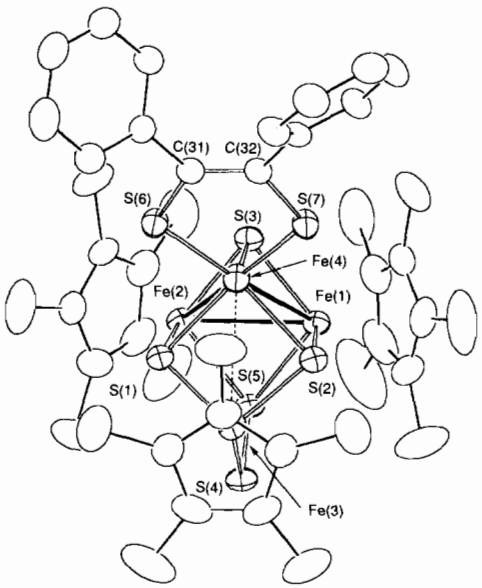

Fig. 4. ORTEP drawing of the cationic moiety in $[5](PF_6)$. Thermal ellipsoids are at 30% probability.

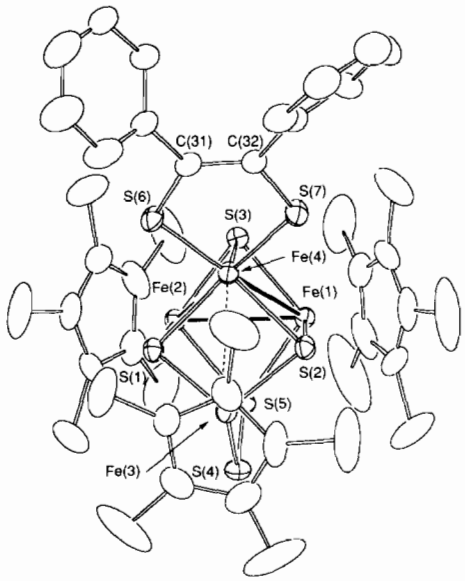

Fig. 5. ORTEP drawing of the dicationic moiety in $[5](PF_6)_2$. Thermal ellipsoids are at 30% probability.

$[(MeC_5H_4)_2Fe](PF_6)$. The dicationic cluster $[Cp'_3(Ph_2C_2S_2)Fe_4S_5](PF_6)_2$ ($[5](PF_6)_2$) was obtained by bulk electrolysis of the monocationic cluster $[5](PF_6)$. The structures of all clusters $[4](PF_6)$, $[5](PF_6)$ and $[5](PF_6)_2$ were determined by X-ray crystallography.

3.3. Structural change of cluster accompanying oxidation of 4 to [4](PF$_6$)

The cubane-type cluster **4** has 18 cluster electrons, so that the total Fe–Fe bond order is three. This was confirmed in the X-ray crystal structure analysis of **4** which revealed that there are three Fe–Fe bonds [13,15]. The structure of the cationic moiety in $[4](PF_6)$ is shown in Fig. 2. Final atomic coordinates and selected interatomic distances and angles are listed in Tables 3 and 4, respectively. Crystalline $[4](PF_6)\cdot CH_2Cl_2$ consists of discrete components of cluster cations, PF_6^- anions and dichloromethane molecules. The symmetry of the Fe_4S_4 core in $[4](PF_6)$ is approximately D_{2d}: the Fe_4S_4 core in $[4](PF_6)$ has four Fe–Fe bonds which make a butterfly-like metal–metal bond framework. A similar distribution of Fe–Fe bonds is also observed in $[Cp_4Fe_4S_4]^{2+}$ [5], $[(MeC_5H_4)_4Fe_4S_4]^+$ [23], $[\{(CF_3)_2C_2S_2\}_4Fe_4S_4]^{2-}$ [24] and $[Cp_4Fe_4Se_4]^n$ ($n = +2$ [7], $+3$ [1]). Four Fe–Fe distances (Fe(1)–Fe(3), Fe(3)–Fe(2), Fe(2)–Fe(4) and Fe(4)–Fe(1)) are much shorter (2.768(1)–2.849(2) Å) than the other two (3.255(2) and 3.222(1) Å). The latter two distances correspond to the absence of Fe–Fe bonds.

The Fe_4S_4 core geometry shows a dramatic change accompanying one-electron oxidation from **4** to $[4]^+$ as shown in Fig. 3. The number of Fe–Fe bonds increases from three to four. The Fe(3)–Fe(4) bond in **4** disappears completely in $[4]^+$ and two new Fe–Fe bonds are created between Fe(2) and Fe(3) and between Fe(1) and Fe(4). According to the metal fragment orbital model [20] and Dahl's MO bonding scheme [5], the total Fe–Fe bond order expected for $[4]^+$ is 3.5. The actual number of Fe–Fe bonds in $[4]^+$ is four and the mean value

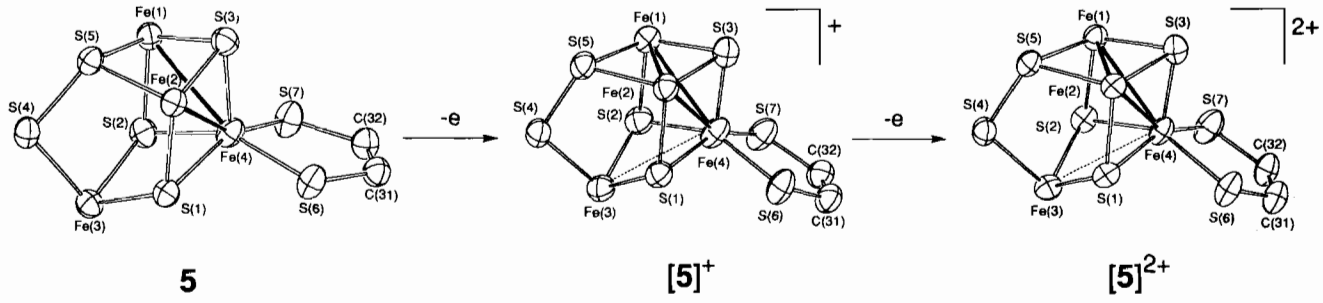

Fig. 6. Structural change of **5** accompanying one- and two-electron oxidation. Cp', Ph groups and counter anions are omitted for clarity.

of the Fe–Fe bond lengths (2.791 Å) is reasonably longer than that of **4** (mean value of three Fe–Fe bonds, 2.739 Å), indicating that the bond order of each of the four Fe–Fe bonds in $[\mathbf{4}]^+$ is less than unity.

3.4. Structural change of clusters accompanying oxidation of 5 to $[5]^+$ and $[5]^{2+}$

The structure of the $[\mathbf{5}]^+$ moiety is shown in Fig. 4. Final atomic coordinates and selected interatomic distances and angles are listed in Tables 5 and 6, respectively. The cationic moiety of cluster $[\mathbf{5}](PF_6)$ has a very similar structure to the parent cluster **5**: the cubane-like Fe_4S_5 core consists of four iron atoms, three μ_3-S ligands and one μ_3-S_2 ligand, and is surrounded by three Cp' ligands and one diphenyldithiolene ligand. The μ_3-S_2 ligand is coordinated to Fe(3) in an 'end-on' mode which has also been found for $[(MeC_5H_4)_4Fe_4S_5](PF_6)$ [21].

The Fe_4S_5 core of **5** has two Fe–Fe bonds in the sequence Fe(1)–Fe(4)–Fe(2) which form a V-shaped configuration [14,15]. On the other hand, in the one-electron oxidized cluster $[\mathbf{5}]^+$, there are three distinct Fe–Fe bonds: the distances Fe(1)–Fe(2), Fe(1)–Fe(4) and Fe(2)–Fe(4) are 2.736(2), 2.783(1) and 2.767(2) Å, respectively. The distances Fe(1)–Fe(3) and Fe(2)–Fe(3) are 3.760(2) and 3.765(2) Å, indicating the absence of Fe–Fe bonds. The distance Fe(3)–Fe(4) is 3.047(2) Å, much shorter than the distances Fe(1)–Fe(3) and Fe(2)–Fe(3) in the same Fe_4S_5 core and the distance Fe(3)–Fe(4) in the parent cluster **5** (3.307(2) Å). Thus, there is some weak Fe–Fe interaction between Fe(3) and Fe(4) in $[\mathbf{5}]^+$.

The structure of the $[\mathbf{5}]^{2+}$ moiety is shown in Fig. 5. Final atomic coordinates and selected interatomic distances and angles for $[\mathbf{5}]^{2+}$ are listed in Tables 7 and 8, respectively. The cluster $[\mathbf{5}]^{2+}$ has a similar structure to $[\mathbf{5}]^+$ and the Fe_4S_5 core contains three distinct Fe–Fe bonds: the distances Fe(1)–Fe(2), Fe(1)–Fe(4) and Fe(2)–Fe(4) are 2.710(1), 2.701(1) and 2.705(1) Å, respectively. There is again weak interaction between Fe(3) and Fe(4) atoms (2.969(1) Å) and the distance is shorter than that in $[\mathbf{5}]^+$. The remaining two distances Fe(1)–Fe(3) and Fe(2)–Fe(3) are 3.728(1) and 3.713(1) Å, indicating the absence of Fe–Fe bonding. The structural change of the Fe_4S_5 core accompanying oxidation of **5** is not simple, as summarized in Fig. 6. This seems to be due to the lowering of cluster symmetry.

5 has 19 cluster electrons. The direct application of the metal fragment orbital model [20] and Dahl's MO bonding scheme [5] predicts that the cluster **5** has a total Fe–Fe bond order of 2.5 [15]. In the actual molecule, there are only two Fe–Fe bonds with a V-shaped configuration as mentioned above, so that each Fe–Fe bond has a bond order of 1.25 [15]. In cluster $[\mathbf{5}]^+$ with 18 cluster electrons, three Fe–Fe bonds are expected to exist. In the actual cluster, a new Fe–Fe bond is created between Fe(1) and Fe(2); hence there are three Fe–Fe bonds with a triangular configuration. However, the Fe(3)–Fe(4) distance in **5** (3.307(2) Å) is shortened to 3.047(2) Å in $[\mathbf{5}]^+$. The structure of $[\mathbf{5}]^{2+}$ is very similar to that of $[\mathbf{5}]^+$, but the distance between Fe(3) and Fe(4) in $[\mathbf{5}]^{2+}$ (2.969(1) Å) is shorter than that in $[\mathbf{5}]^+$ (3.047(2) Å).

The averaged distances of the six Fe–Fe bonds for each of the clusters **5**, $[\mathbf{5}]^+$ and $[\mathbf{5}]^{2+}$ are 3.26, 3.14 and 3.09 Å, respectively. In other words, the Fe_4 core of **5** shrinks with each increase in charge of the cluster and this indicates that oxidation of **5** causes the stepwise removal of antibonding electrons from the neutral cluster.

The mean Fe–S bond distances in the Fe_4S_4 core of **4** (2.22 Å) and in the Fe_4S_5 core of **5** (2.21 Å) remain unchanged upon oxidation of the clusters.

In all clusters, **4**, $[\mathbf{4}]^+$, **5**, $[\mathbf{5}]^+$ and $[\mathbf{5}]^{2+}$, it was observed that the Fe–S(dithiolene) distances are shorter than the Fe–S distances in the Fe_4S_4 and Fe_4S_5 cores. This suggests that the Fe–S(dithiolene) bonds have some unsaturated bonding character. Similar findings have been reported for $[\{(CF_3)_2C_2S_2\}_4Fe_4S_4]^{2-}$ [24], $[Fe_2\{S_2C_2(CF_3)_2\}_4]^-$ [25] and $Fe\{S_2C_2(CF_3)_2\}(S_2CNEt_2)_2$ [26].

4. Supplementary material

Complete atom-labeling schemes for [4]$(PF_6)\cdot CH_2Cl_2$, [5]$(PF_6)\cdot 2Me_2CO$ and [5]$(PF_6)_2\cdot Me_2CO$, tables of detailed crystallographic data, atomic coordinates and thermal parameters, bond distances and angles, and listings of observed and calculated structure factors for [4]$(PF_6)\cdot CH_2Cl_2$, [5]$(PF_6)\cdot 2Me_2CO$ and [5]$(PF_6)_2\cdot Me_2CO$ are available from the authors on request.

Acknowledgement

This work was supported by a Grant-in-Aid for Scientific Research (No. 05209203) from the Ministry of Education, Science and Culture of Japan.

References

[1] H. Ogino, H. Tobita, K. Yanagisawa, M. Shimoi and C. Kabuto, *J. Am. Chem. Soc., 109* (1987) 5847.
[2] H.L. Blonk, J.G.M. van der Linden, J.J. Steggerda and J. Jordanov, *Inorg. Chim. Acta, 158* (1989) 239.
[3] (a) R.A. Schunn, C.J. Fritchie, Jr. and C.T. Prewitt, *Inorg. Chem., 5* (1966) 892; (b) C.H. Wei, G.R. Wilkes, P.M. Treichel and L.F. Dahl, *Inorg. Chem., 5* (1966) 900.
[4] Trinh-Toan, W.P. Fehlhammer and L.F. Dahl, *J. Am. Chem. Soc., 99* (1977) 402.
[5] Trinh-Toan, B.K. Teo, J.A. Ferguson, T.J. Meyer and L.F. Dahl, *J. Am. Chem. Soc., 99* (1977) 408.
[6] H. Ogino, A. Satoh and M. Shimoi, *Bull. Chem. Soc. Jpn., 63* (1990) 2314.
[7] R.M. Roder, *Ph.D. Thesis,* University of Wisconsin-Madison, Madison, WI, 1973.
[8] C.R. Szmanda, *Ph.D. Thesis,* University of Wisconsin-Madison, Madison, WI, 1979.
[9] G.J. Kubas and P.J. Vergamini, *Inorg. Chem., 20* (1981) 2667.
[10] P.J. Vergamini and G.J. Kubas, *Prog. Inorg. Chem., 21* (1967) 261.
[11] N. Dupré, H.M.J. Hendriks, J. Jordanov, J. Gaillard and P. Auric, *Organometallics, 3* (1984) 800.
[12] N. Dupré, P. Auric, H.M.J. Hendriks and J. Jordanov, *Inorg. Chem., 25* (1986) 1391.
[13] S. Inomata, H. Tobita and H. Ogino, *J. Am. Chem. Soc., 112* (1990) 6145.
[14] S. Inomata, H. Tobita and H. Ogino, *Inorg. Chem., 31* (1992) 722.
[15] S. Inomata, K. Hiyama, H. Tobita and H. Ogino, *Inorg. Chem., 33* (1994) in press.
[16] (a) D.N. Hendrickson, Y.S. Sohn and H.B. Gray, *Inorg. Chem., 10* (1971) 1559; (b) D.M. Duggan and D.N. Hendrickson, *Inorg. Chem., 14* (1975) 955.
[17] *International Tables for X-ray Crystallography,* Vol. IV, Kynoch, Birmingham, UK, 1974, Table 2.2A, pp. 72–98; Table 2.3.1, pp. 149–150.
[18] R.F. Stewart, E.R. Davidson and W.T. Simpson, *J. Chem. Phys., 42* (1965) 3175.
[19] T. Sakurai and K. Kobayashi, *Rikagaku Kenkyuusho Houkoku, 55* (1979) 69.
[20] S. Harris, *Polyhedron, 8* (1989) 2843.
[21] H.L. Blonk, J. Mesman, J.G.M. van der Linden, J.J. Steggerda, J.M.M. Smits, G. Beurskens, P.T. Beurskens, C. Tonon and J. Jordanov, *Inorg. Chem., 31* (1992) 962.
[22] A.L. Balch, *J. Am. Chem. Soc., 91* (1969) 6962.
[23] H.L. Blonk, J.G.M. van der Linden, J.J. Steggerda, R.P. Geleyn, J.M.M. Smits, G. Beurskens, P.T. Beurskens and J. Jordanov, *Inorg. Chem., 31* (1992) 957.
[24] T.H. Lemmen, J.A. Kocal, F.Y.-K. Lo, M.W. Chen and L.F. Dahl, *J. Am. Chem. Soc., 103* (1981) 1932.
[25] A.J. Schultz and R. Eisenberg, *Inorg. Chem., 12* (1973) 518.
[26] D.L. Johnston, W.L. Rohrbaugh and W. Dew. Horrocks, Jr., *Inorg. Chem., 10* (1971) 1474.